



OPEN Oxidative stress in a cellular model of alcohol-related liver disease: protection using curcumin nanoformulations

Lucy Petagine¹, Mohammed G. Zariwala¹, Satyanarayana Somavarapu², Stefanie Ho Yi Chan^{1,2}, Evrim A. Kaya¹ & Vinood B. Patel¹✉

Alcohol-related liver disease (ARLD) is a global health issue causing significant morbidity and mortality, due to lack of suitable therapeutic options. ARLD induces a spectrum of biochemical and cellular alterations, including chronic oxidative stress, mitochondrial dysfunction, and cell death, resulting in hepatic injury. Natural antioxidant compounds such as curcumin have generated interest in ARLD due to their ability to scavenge reactive oxygen species (ROS), however, therapy using these compounds is limited due to poor bioavailability and stability. Therefore, the aim of this study was to assess the antioxidant potential of free antioxidants and curcumin entrapped formulations against oxidative damage in an ARLD cell model. HepG2 (VL-17A) cells were treated with varying concentrations of alcohol (from 200 to 350 mM) and parameters of oxidative stress and mitochondrial function were assessed over 72 h. Data indicated 350 mM of ethanol led to a significant decrease in cell viability at 72 h, and a significant increase in ROS at 30 min. A substantial number of cells were in late apoptosis at 72 h, and a reduction in the mitochondrial membrane potential was also found. Pre-treatment with curcumin nanoformulations increased viability, as well as, reducing ROS at 2 h, 48 h and 72 h. In summary, antioxidants and entrapped nanoformulations of curcumin were able to ameliorate reduced cell viability and increased ROS caused by ethanol treatment. This demonstrates their potential at mitigating oxidative damage and warrants further investigation to evaluate their efficacy for ARLD therapy.

Keywords Alcohol, Antioxidants, Curcumin, Liver, Mitochondria, Oxidative stress, Reactive oxygen species

Alcoholic related liver disease (ARLD) is a progressive chronic disease which develops due to excessive and prolonged alcohol exposure resulting in steatosis, alcoholic hepatitis, fibrosis/cirrhosis and in some cases, hepatocellular carcinoma¹. Liver disease is a significant global health issue, responsible for around two million deaths per year and 4% of all deaths worldwide². The World Health Organization's (WHO) Global Status Report on Alcohol and Health estimates 2.3 billion people currently consume alcohol, with an average intake daily of 32.8 g of alcohol per person³. Multiple factors have been identified as inducers of liver inflammation in response to alcohol. These factors include mitochondrial dysfunction, gut dysbiosis, alcohol metabolites, necrotic cell products such as damage associated molecular patterns (DAMPs), apoptosis and mitophagy⁴. These factors are highly interactive with common downstream intermediates, in particular, reactive oxygen species (ROS), which results in a state of oxidative stress⁵. Furthermore, the highly reactive by-product of alcohol metabolism, acetaldehyde, can form protein and DNA adducts, generate ROS, and stimulate an immune response^{6–9}, thus promoting inflammation. Disruption to the mitochondrial electron transport chain (ETC) and oxidative phosphorylation is also a common feature in ARLD, leading to necroptosis^{10,11}. However, the exact mechanisms of inflammation, mitochondrial dysfunction and pro-inflammatory cytokines production requires further research^{12,13}.

Abstaining from alcohol is considered the primary therapeutic approach for individuals attending rehabilitation centres^{1,14}, where abstinence from alcohol has demonstrated a reduction in portal pressure, a decreased likelihood of advancing to cirrhosis, and an improvement in survival rates^{14,15}. Unfortunately,

¹Centre for Nutraceuticals, School of Life Sciences, University of Westminster, 115 New Cavendish Street, London W1W 6UW, UK. ²Department of Pharmaceutics, UCL School of Pharmacy, London, UK. ✉email: v.b.patel@westminster.ac.uk

abstaining from alcohol has high relapse rates, ranging from 67 to 81% among alcoholics¹⁶. Research has also shown that 60% of patients with alcohol use disorder will relapse within 6 months. Furthermore, limited therapeutic options exist for the treatment of severe alcoholic hepatitis which has a mortality rate of up to 45%¹⁷ and limited studies exist which indicate improvement in survival rates amongst alcoholic hepatitis patients^{18,19}. Clinical trials for ARLD have not been successful, including the highly anticipated Steroids or Pentoxifylline for Alcoholic Hepatitis (STOPAH) trial^{20,21}. Other clinical trials for ARLD which have not been successful; include IFN- γ , angiotensin II antagonists and IL-10²². Therefore, this highlights the need for alternative treatment approaches capable in mitigating oxidative stress and liver injury, a critical step in disease pathology.

Glutathione (GSH) is the main cellular antioxidant synthesised by S-adenosyl methionine (SAM) and can control cellular redox and protect against oxidative stress, neutralising ROS, however, during ARLD development, GSH levels are depleted. Antioxidant therapy has been considered useful for ARLD treatment as many antioxidant compounds can mediate ROS including vitamins E and C, N-acetylcysteine (NAC), SAM, and betaine^{9,23}. Curcumin has also been shown to have antioxidant properties and can reduce oxidative stress via ROS reduction in animal models²⁴. Although curcumin possesses beneficial antioxidant properties it has low bioavailability and stability issues, therefore, the ability to achieve targeted therapeutic doses becomes limited. Nanoformulations may mitigate some difficulties faced with traditional drugs due to their ability to deliver drugs to specific cell types based on surface receptor binding²², as well as controlled drug release, specific cell penetration, improved pharmacokinetics, and reduced side effects²⁵. Novel nanocarrier delivery systems entrapping curcumin have previously been shown to protect against oxidative stress in a Parkinson's disease model²⁶.

The combination of entrapped antioxidants for the treatment of ARLD may provide a promising approach compared to traditional treatments in the ability to reduce oxidative stress. Therefore, the aim of this study was to utilise novel nanocarrier systems entrapping potent antioxidants such as curcumin to assess their ability to protect against ethanol induced damage in a liver cell model.

Materials and methods

Cell culture

HepG2 (VL-17A) cells (kindly provided by Dr Clemens, University of Nebraska) which overexpress both ADH and CYP2E1 were cultured in Dulbecco's Modified Eagles Medium (Lonza Ltd, UK) supplemented with 10% foetal calf serum (FCS) (Gibco, UK)^{27–31}, 10 U/mL penicillin/streptomycin, 2 mM L-glutamate and 50 μ g/mL gentamycin sulphate (Lonza, UK), which has been previously characterised when studying fatty liver and alcohol toxicity mechanisms^{31–34}. When cells reached 70% confluency, they were passaged using a 0.5 \times trypsin solution in phosphate buffered saline (PBS) and viability of cells was assayed using trypan blue.

Cell treatments

Cells were seeded according to the appropriate protocol (as described below) and treated with varying concentrations of ethanol (100, 200 mM, 300 mM, 350 mM) in low glucose (1.0 g/L) DMEM supplemented with 1% (v/v) foetal calf serum (FCS), 1% penicillin/streptomycin (100 U/mL) and 1% L-Glutamine (2 mM).

These alcohol concentrations were chosen, as we have previously shown that in HepG2 cells that overexpress ADH, 100 mM alcohol treatment led to a moderate decrease in cell viability and mitochondrial function³⁴. As a consequence, to induce more cellular injury that reflects severe alcoholic hepatitis, higher alcohol concentrations were characterized up to 350 mM. The concentration is in alignment with other *in vitro* studies using HepG2 cells from 171 to 750 mM^{27,35–37}; 100–800 mM in a L-02 hepatocyte line³⁸, 200 mM in a mouse liver cell line³⁹, 300 mM in neuronal cells⁴⁰. For cell culture, the original methodology as stated by Clemens et al., was followed where flasks were tightly sealed or cell culture plates were sealed to prevent ethanol evaporation^{29,41}. To determine whether nanocarrier systems could protect against oxidative damage VL17-A cells were also treated with antioxidant compounds and the above nanoformulations (produced in collaboration with UCL) at differing concentrations and time points as either a pre-treatment prior to ethanol or, added as co-treatment with ethanol. The varying treatments were studied using parameters of liver toxicity over 30 min to 72 h. The effects of cell treatment were assessed by the methods below.

Cell viability

Cells were seeded at 1×10^4 cell/well and incubated overnight to allow attachment. Following treatment, 5 mg/mL 3-(4,5-Dimethylthiazol-2-yl)-2,5-diphenyltetrazolium bromide (MTT) was added to each well and incubated at 37 °C for 2 h³¹. After incubation, the reagent was removed, and cells were incubated with 100 μ L/well DMSO for 15 min at room temperature. The plates were then measured at 550 nm.

Reactive oxygen species assay

The level of ROS production was assayed using a method adapted from Baldini et al.⁴². Cells were seeded at 1×10^4 cell/well and incubated overnight to allow attachment. Following treatment, the cells were washed twice with PBS and incubated with 200 μ L of 200 μ M 2, 7-dichlorofluoresceindiacetate (DCF-DA) (Sigma, UK) and incubated at 37 °C for 30 min in the dark. Following incubation, the substrate solution was removed, and cells were washed in PBS. 200 μ L of PBS was then added to each well and fluorescence was measured at excitation 485 nm and emission 535 nm.

Measurement of apoptosis

To determine quantities of apoptotic cells after treatment, the Annexin VFITC/propidium iodide (PI) staining kit (BioLegend, UK) was used to stain cells and measured by flow cytometry. 3×10^5 cells were seeded in 12-well plates and left overnight to attach. Cells were treated as described above over 72 h. After treatment, supernatant

of cells was kept, and cells were then washed with PBS prior to detachment from plates with 200 μL trypsin (incubated at 37 °C for 5 min). After detachment, 800 μL of 10% FCS DMEM was then added to neutralise the trypsin and the cell/supernatant mixture was then centrifuged at 400 g for 5 min. Cell pellets were resuspended in 500 μL of 1X Annexin V Binding Buffer and stained with 5 μL of Annexin V-FITC and 5 μL PI and analysed on the BD LSRFortessa™ (Ex = 488 nm, Em = 530 nm) using the FACSDiva software.

Measurement of mitochondrial respiration

HepG2 cells were plated in 24-well Seahorse MitoStress Assay cell plates at a density of 2×10^4 cells per well. Cells were then treated with the previously described conditions of alcohol. After the defined treatment length, cells were washed with Seahorse Assay Medium (pH 7.4) containing 25 mM glucose and 1mM sodium pyruvate³¹. MitoStress drugs oligomycin (4 μM), FCCP (4 μM), and antimycin/Rotenone mixture (2.5 μM) were added, and the oxygen consumption rate (OCR) was measured using the Seahorse XFE Flux Analyzer under basal conditions. OCR values were normalised to total protein content which was measured using the Bradford Assay⁴³ (Bio-Rad Laboratories, UK).

Measurement of genome damage

The cytokinesis-block micronucleus cytochrome assay was performed as described by Michael Fenech⁴⁴ to analyse measures of genome damage and chromosomal instability. 1×10^5 cells were seeded in T25 flasks, and the following day treated as described above. Cytochalasin B was added to media for 24 h prior to their fixation. Following this, cells were then detached from flasks using trypsin and centrifuged at 400 g. After centrifugation, the supernatant was discarded and then replaced with 7 mL prewarmed 0.075 M potassium chloride and incubated at 37 °C for 7 min. Cells were then centrifuged and potassium chloride was removed and replaced with 5 mL fixative (methanol:acetic acid (3:1)). For analysis, cells were centrifuged and resuspended in 500 μL cold fixative and dropped onto microscope slides then stained with DAPI and 5% Giemsa. The number of micronuclei (MNi), nucleoplasmic bridges (NPBs), and nuclear buds (NBUDs) were scored from 100 binucleated cells.

Preparation of antioxidant nanoformulations

The concentrations of curcumin (5 and 10 μM) used in this study were optimised based on previous studies from our research group^{26,45} and existing literature^{46,47}. Concentrations of 5 μM and 10 μM have been found to serve as the optimal concentration in preclinical studies for assessing absorption efficiency and assessing the potential of bioenhancement strategies, such as nanoformulations and liposomal encapsulations. Determining the pharmacokinetic profile at 5 μM and 10 μM concentrations helps define the therapeutic window of curcumin, which can potentially identify the minimum effective concentration needed to produce a pharmacological effect. These optimised concentrations were thus chosen to ensure measurable and reproducible effects while minimising cytotoxicity.

All nanoformulations were prepared using a modified thin-film hydration method^{48,49}. Curcumin entrapment in nanoformulations were prepared with 100% DSPE-PEG^{50,51}. A rotary evaporator (Buchi Rotavapor® R-100, Flawil, Switzerland) was then used to evaporate the methanol (200 rpm and 80 °C), under vacuum^{45,52–54}. Once a thin film was achieved, it was then hydrated with 10 mL of Milli-Q water and mixed at 80 °C then sonicated using a VWR Ultrasonic cleaner bath USC300T (VWR International Limited, UK) for a further 5 min^{45,52–54}. The solution was then filtered through a sterile 0.45 μm filter to remove any unloaded antioxidants^{45,52–54}.

Size and surface charge of nanoformulations

The size and surface charge of nanoformulations were measured by dynamic light scattering (DLS) as Z_{Ave} hydrodynamic diameter, polydispersity index (PDI) and zeta potential (ζ), using the Zetasizer Nano ZS (Malvern Instruments, UK)^{45,52–54}. 1 mL of the nanoformulated sample was pipetted into the zeta potential DTS1070 folded capillary cell (Malvern Panalytical, UK). Zeta potential was calculated via electrophoretic mobility using Malvern data analysis software following the Helmholtz-Smoluchowski equation^{45,52–54}.

Determination of drug loading and entrapment efficiency

Drug loading and entrapment efficiency of nanoformulations were measured by UV-Visible spectrophotometer (Cary Series UV-Vis spectrophotometer, Agilent Technologies, USA) using free drug calibration curves^{45,52–54}. Curcumin was measured at 424 nm. The percentage of drug loading and entrapment efficiency were calculated using the following equations⁵⁴:

$$\text{Drug loading (\%)} = \frac{\text{total weight of entrapped drug}}{\text{total weight of all raw materials}} \times 100$$

$$\text{Encapsulation efficiency (\%)} = \frac{(\text{determined mass of drug entrapped within nanocarriers})}{\text{actual mass of drug}} \times 100$$

Statistical analysis

Results were analysed using either one or two-way ANOVA. Statistical analysis was followed by Tukey's multiple comparisons post hoc test. Data is expressed as mean + standard error of the mean (SEM) and P values ≤ 0.05 were considered statistically significant.

Results

HepG2 (VL-17A) cells were exposed to varying concentrations of ethanol (100–400 mM) and cell viability was assessed. At 48 h, an 18% decrease in cell viability was observed after 300 mM ethanol exposure, 350 mM ethanol

led to a 31% decrease ($p=0.0005$) and 400 mM also led to a 37% decrease ($p<0.0001$) (Fig. 1). Ethanol toxicity was most apparent after 72 h whereby 300 mM alcohol led to a 27% decrease ($p=0.0438$), 350 mM led to a 50% decrease ($p<0.0001$) and 400 mM a 63% decrease ($p<0.0001$) (Fig. 1C).

At 30 min, a 25% increase in ROS was seen after treatment with 300 mM and a 53% increase ($p=0.0027$) after treatment with 350 mM ethanol (Fig. 2). Similarly, at 72 h, 200 mM ethanol exposure increased ROS by 42%, and 300 mM increased ROS by 96% ($p=0.0005$) (Fig. 2F). At 48 h, the percentage of cells in early apoptosis also increased significantly with 20% ($p=0.0313$) of cells treated with 350 mM ethanol in early apoptosis (Fig. 3). Overall, at 72 h, both the percentage of early and late apoptosis was highest, and 350 mM ethanol caused 44% of cells to undergo late apoptosis ($p=0.0153$) (Fig. 3). A dose dependent decrease in mitochondrial membrane potential was also observed across all time points (Fig. 4). Mitochondria play a crucial role in ROS formation and cellular energy metabolism and recent research indicates that alcohol consumption can induce alterations in both the structure and function of mitochondria. The assessment of mitochondrial respiratory function was conducted by measuring the OCR (Supplementary Fig. S1). At 24 h, measurements of oxygen consumption were also reduced (Supplementary Fig. S2). Preliminary findings indicate that ethanol treatment leads to an increase in measures of chromosomal instability, with significant increases in NBUD formation (Supplementary Fig. S4).

Free drug curcumin was tested in its ability to prevent cellular injury due to alcohol. At 48h, 200 mM ethanol led to a 22% reduction in viability, 300 mM led to a 53% reduction and 350 mM led to a 75% reduction in viability and at 72 h mM ethanol led to a 52% reduction in viability and 300 mM and 350 mM both led to a 95% reduction in viability. 5 μ M and 10 μ M curcumin were assessed, and this data shows that when curcumin was included with ethanol it provided protection against ethanol and induced damage to HepG2 cells. At 48 h, 5 μ M free drug was able to increase viability by 237% with 300 mM ethanol ($p=0.0030$) and 369% with 350 mM ethanol ($p=0.0141$), when compared to the ethanol treated only controls (Fig. 5). At 72 h, 5 μ M free drug was able to increase viability by 88% with 200 mM ethanol ($p=0.0335$), 1650% with 300 mM ethanol ($p=0.0002$), and 1933% with 350 mM ethanol ($p<0.0001$), when compared to the ethanol treated only controls (Fig. 5). 10 μ M free drug was able to increase viability by 139% with 200 mM ethanol ($p=0.0008$), 2014% with 300 mM ethanol ($p<0.0001$), and 1100% with 350 mM ethanol ($p=0.0052$), when compared to the ethanol treated only controls (Fig. 5).

Novel nanocarrier delivery systems for the antioxidant curcumin were used to assess their ability in the protection against ethanol induced changes in VL-17A cells. Formulations of curcumin DSPE-PEG nanoformulation exhibited notably high encapsulation efficiency, ranging from 74 to 78% (Table 1). The average particle sizes of the nanoformulation, as measured by diameter, were consistently below 10 nm. Specifically, the mean diameter for DSPE-PEG nanocarrier was 8.40 nm and the polydispersity index (PDI) values, reflecting the heterogeneity of nanocarrier solutions, were low (<0.5). The evaluation of Zeta Potential (mV) was employed to assess the surface charge of the nanoformulations. Nanocarriers exhibited comparable low negative surface charges, measuring -15.20 mV.

Protection with curcumin formulated in DSPE-PEG carrier was assessed using MTT assay (Fig. 6). At 48 h, 350 mM ethanol caused a reduction in cell viability by 45%. Pre-treatment with 10 μ M curcumin DSPE-PEG increased viability by 24% when compared to 350 mM ethanol treatment alone (Fig. 6). At 72 h, 350 mM ethanol caused a reduction in cell viability by 50%. Pre-treatment with 10 μ M curcumin DSPE-PEG increased viability by 27% when compared to 350 mM ethanol treatment alone (Fig. 6).

Curcumin DSPE-PEG nanoformulations were shown to protect VL-17A cells against ROS production (Figs. 7, 8). At 30 min, pre-treatment with 10 μ M curcumin DSPE-PEG reduced ROS by 26% and at 1 h, 10 μ M curcumin DSPE-PEG a 20% reduction was observed, compared to corresponding ethanol only treatment. At 2

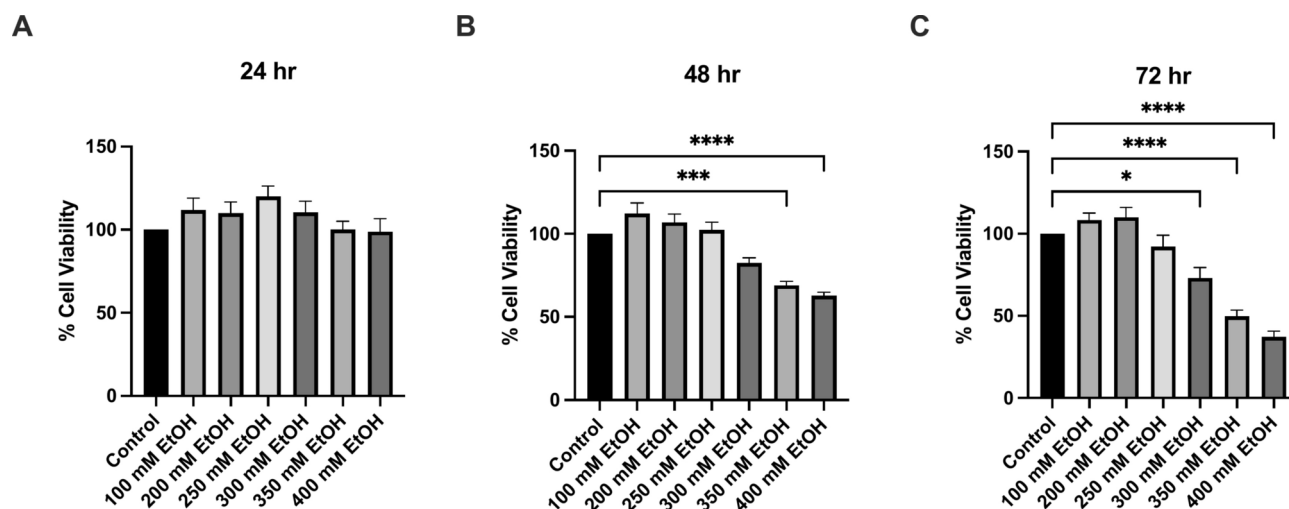


Fig. 1. The effect of ethanol exposure on cell viability at (A) 24 h, (B) 48 h and (C) 72 h. Data is presented as percentage from the control. Results presented as mean of replicates \pm SEM ($n=9$) * $P\leq 0.05$, *** $P\leq 0.001$, **** $P\leq 0.0001$.

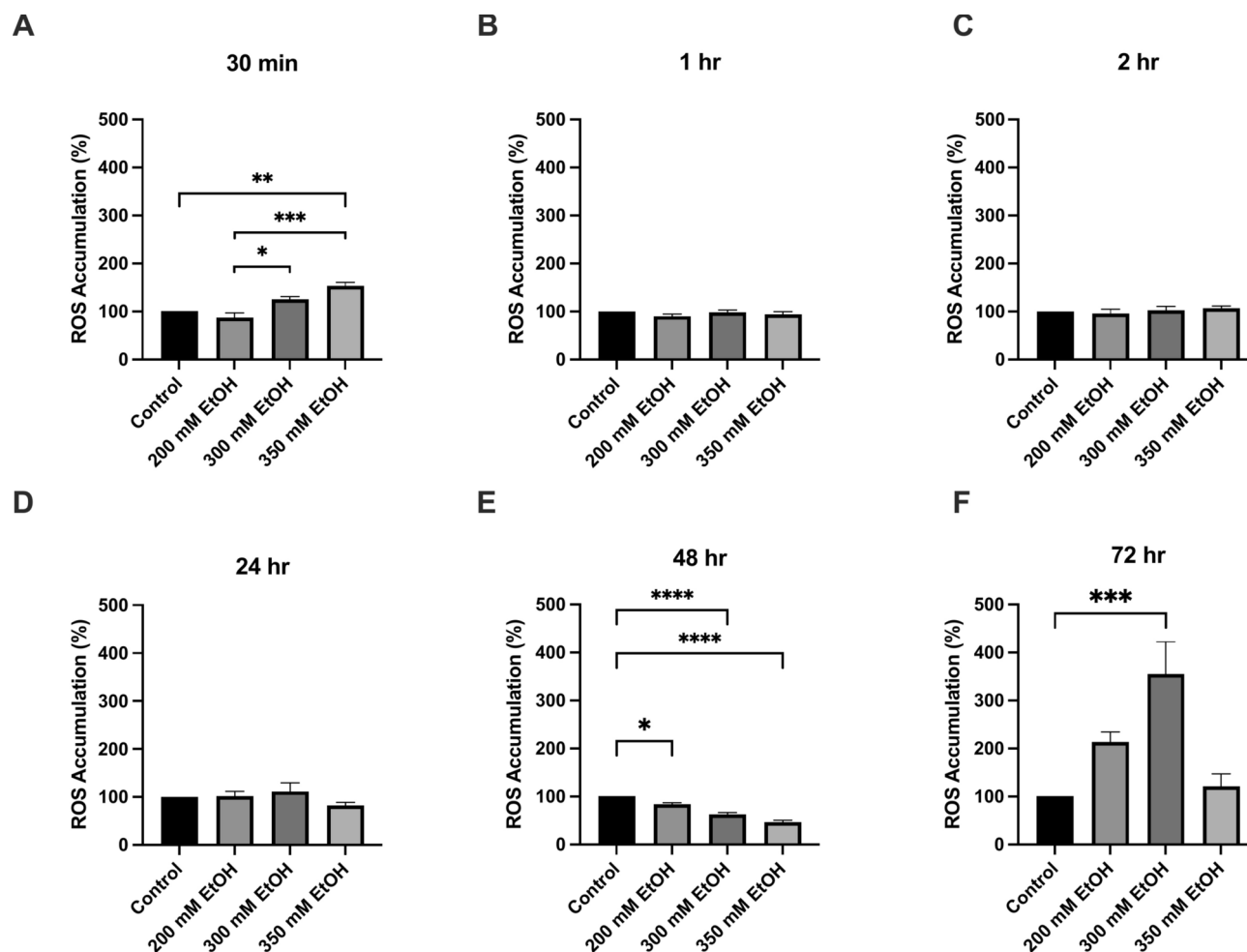


Fig. 2. The effect of alcohol exposure on ROS accumulation at (A) 30 min, (B) 1 h, (C) 2 h, (D) 24 h, (E) 48 h and (F) 72 h. Cells were seeded in 96-well plates and treated with 200 mM, 300 mM, and 350 mM ethanol. Data is presented as percentage from the control. Results are expressed as mean of replicates \pm SEM (n = 3–6). *P \leq 0.05, **P \leq 0.01, ***P \leq 0.001, ****P \leq 0.0001.

h, pre-treatment with 10 μ M curcumin DSPE-PEG reduced ROS by 29%. At 48 h, pre-treatment with 10 μ M curcumin DSPE-PEG reduced ROS by 36% (p = 0.0226) and at 72 h pre-treatment with 10 μ M curcumin DSPE-PEG significantly reduced ROS by 51% (p = 0.0013).

Discussion

ARLD is a significant global health issue, however, the precise mechanisms for liver injury are still incompletely understood. This in part explains the limited treatment options available, particularly for acute alcoholic hepatitis which has a 60-day mortality rate of 20–30%⁵⁵, which increases to 40% at 180 days after admission¹⁷. We have previously shown that 100 mM ethanol in HepG2 cells causes a moderate decrease in cell viability and mitochondrial function (loss in membrane potential and lower ATP levels)³⁴. This suggested that higher ethanol concentrations were required to induce more pronounced cellular injury, and thus we could evaluate the antioxidant properties of nanoformulations under more damaging conditions that reflects severe alcoholic hepatitis. This is similar to other models of ARLD, where liver slices were exposed to 250 mM and 500 mM ethanol⁵⁶.

In this study, HepG2 (VL-17A) cells were used as a model to investigate alcohol-induced injury in liver cells in relation to oxidative stress, apoptosis, mitochondrial dysfunction, and genomic damage. Ethanol treatment led to significant cell toxicity, indicating a correlation between alcohol dosage and reduced cell viability over time. This study also found increased levels of ROS and apoptosis as well as decreases in mitochondrial membrane potential, suggesting ethanol treatment causes oxidative stress as well as disrupts mitochondrial cellular energy production, which in turn, causes activation of apoptosis. Results also show ethanol treatment leads to chromosomal instability and genome damage.

Mitochondrial dysfunction occurs due to the increase in ROS production and oxidative stress. During alcohol metabolism, excess NADH is produced which alters the cellular redox status and drives complex I of the ETC, causing electron leakage from complexes I and III, and the generation of superoxide anion radical and hydrogen

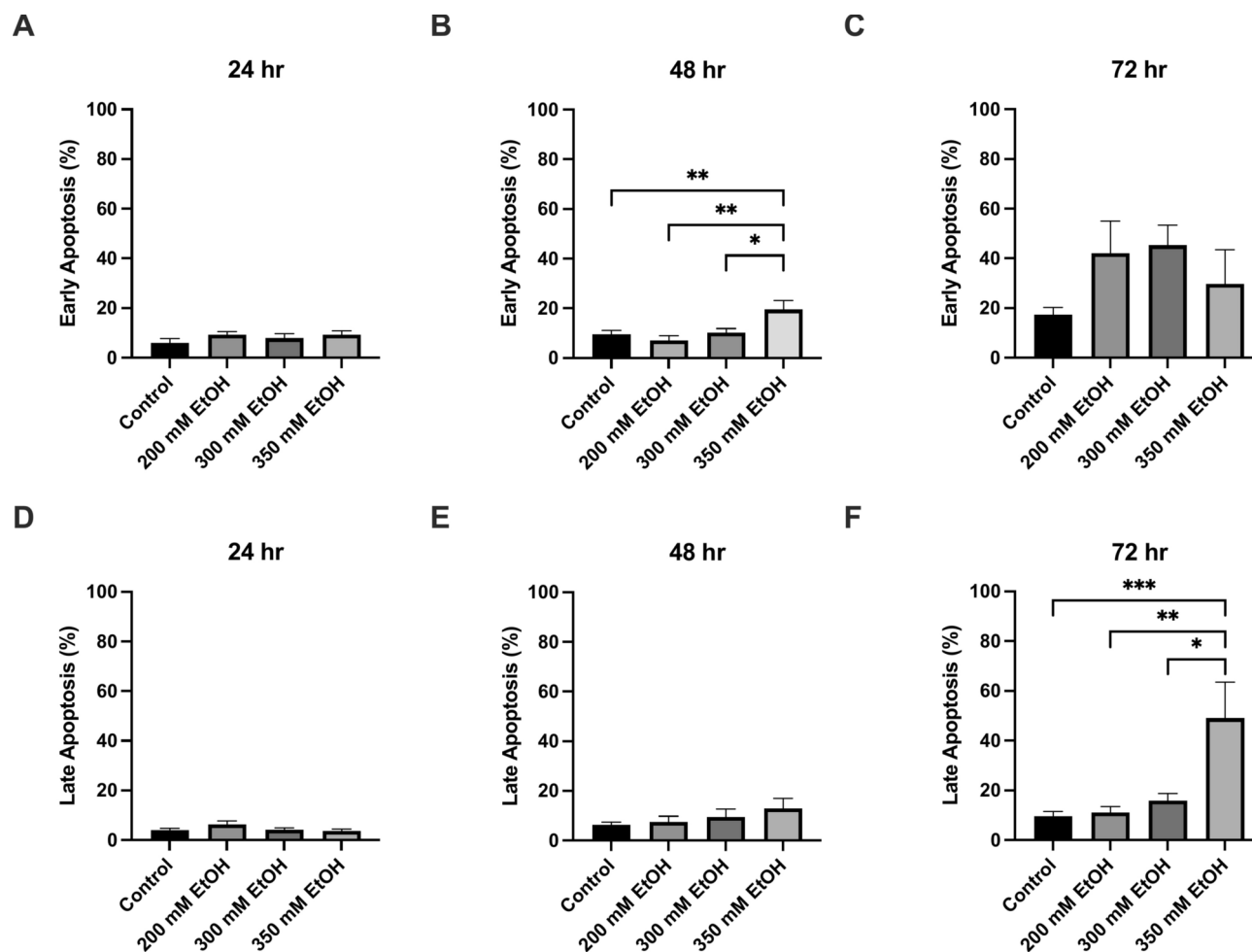


Fig. 3. The effect of ethanol exposure on apoptosis (A) 24 h early apoptosis (B) 48 h early apoptosis, (C) 72 h early apoptosis, (D) 24 h late apoptosis (E) 48 h late apoptosis, (F) 72 h late apoptosis. Data is presented as percentage of positive cells. Results presented as mean of replicates \pm SEM (n = 3–10). *P \leq 0.05, **P \leq 0.01, ***P \leq 0.001.

peroxide^{9,57–60}. *In-vivo*, alcohol has also been shown to increase gut dysbiosis, causing LPS translocation and production of pro-inflammatory cytokines such as TNF- α , and IL-8, which in turn, can induce apoptosis^{9,61}. Apoptosis can also be induced due to protein adduct formation which elicits an immunological response and production of IFN- γ and TNF- α ⁶¹. Induction of apoptosis may also occur due to hypoxia and reduced levels of mitochondrial GSH⁶². Therefore, increases observed in apoptosis may be due to the reduction in mitochondrial membrane potential, dysfunctional cellular redox status and reduced levels of antioxidants.

In the present study an increase in late apoptosis was observed. The late phase of apoptosis is marked by DNA fragmentation, as well as morphological and phenotypic changes. Previous research has shown that ethanol treatment causes increases in DNA fragmentation⁶³ as well as DNA damage and chromosomal and genomic instability^{64,65}, which has been confirmed by the present study regarding ethanol and genomic instability.

It is well known that excessive alcohol causes oxidative stress and DNA damage. When DNA damage occurs, chromosomal and genomic instability can increase which leaves cells susceptible to oxidative stress, inflammation and cancer⁶⁴. Data in this study shows that treatment with various concentrations of ethanol causes increased numbers of micronuclei and nuclear buds, suggesting excessive alcohol treatment may induce cancer initiation via DNA damage⁶⁴. Although the mechanisms are not well known, acetaldehyde, the toxic by-product, can bind to DNA producing point mutations⁶⁶. In addition, acetaldehyde disrupts mitochondrial GSH uptake, electron transport chain activity and directly impairs mitochondrial respiration^{67–69}.

Whilst most of the toxicity arose at the latter time points, it is important to demonstrate in the current study the transitional dose and time dependent effects of alcohol treatment from 24 to 72 h. It is likely the initial increase in ROS production, arises due to immediate alcohol metabolism, whereas there is a lag time in cellular injury, with minimal changes in viability occurring at 24 h, and viability decreasing at latter time points 48–72 h. We have previously reported that *in-vivo*, alcohol toxicity occurs over a 24–72 h period in the hepatic cytosol and mitochondria, with specific changes in oxidative stress. Furthermore, acetaldehyde causes further detrimental effects over the 72 h period⁶⁸, highlighting the differential time dependent effects of alcohol and acetaldehyde.

Due to the significant contribution of oxidative stress to the inflammatory process in ARLD, antioxidant therapy has been considered as a treatment approach. There is substantial evidence supporting the protective effects of curcumin in many disorders including neurological disease, liver disease, cancer, diabetes and cardiovascular diseases^{70–73}. However, the use of these antioxidants for potential therapy has been hindered by their low bioavailability, low stability and low concentration at the target site. Nanomedicine is an emerging technology which offers promising solutions to these problems as they can preserve the potency of the entrapped compound while improving targeted delivery and crossing biological membranes.

Novel nanocarrier delivery systems have become of recent interest as they aim to enhance stability, bioavailability, and delivery of the entrapped compounds to specific cells. Formulations have also been developed to increase solubility⁷⁴. The aim of this study was to use DSPE-PEG nanocarrier systems to entrap potent antioxidant compounds such as curcumin to assess their ability in protecting against oxidative stress in ARLD. Curcumin has previously been shown to exhibit its antioxidant, anti-inflammatory and anticarcinogenic property on the liver. Previous research has shown that hydrogen peroxide treatment on HepG2, inducing oxidative stress, can be mitigated by the effects of curcumin which was shown to reduce ROS and malondialdehyde (MDA) formation (a by-product of lipid peroxidation), as well as increase antioxidant enzyme capacity such as superoxide dismutase and catalase⁷⁵.

Concentrations of nanocarriers were used at a dose of 10 μM , in accordance with previously published data from our group^{26,45,52}. Free drug curcumin was shown to significantly increase viability of cells treated with varying concentrations of ethanol across all concentrations and time points. Curcumin free drug co-treatment at both 5 μM and 10 μM concentrations were able to completely ameliorate loss of viability caused by ethanol back to control levels in some cases. Across both time points, curcumin DSPE-PEG nanocarriers were able to protect to at least the same extent as the free drug against the ethanol induced loss of cell which suggests 3 h pre-treatment of 10 μM curcumin DSPE-PEG could be protective against oxidative stress and liver injury in ARLD. Curcumin DSPE-PEG nanocarriers were also able to protect against ROS production. The specific mechanisms of action behind the novel nanocarriers are complex however, it is thought that their effects are due to modulation of antioxidant signalling and mitochondrial function.

Previous research has suggested that treatment with curcumin may alter pathways associated with liver disease such as TGF- β 1/Smad, JNK1/2-ROS, NF- κ B as well as antioxidant signalling⁷⁶. Curcumin mechanisms of action may also be due to the pentose-phosphate pathway. The pentose-phosphate pathway functions to supply NADPH which is required for conversion of oxidised GSH to reduced GSH via glutathione reductase^{60,77}. Therefore, it is possible that the ability of entrapped curcumin to protect against ethanol may be due to their potential in increasing intracellular GSH. In support of this, we have previously used *N*-acetylcysteine formulations in a model of Parkinsons disease²⁶, where a reduction in oxidative stress was observed. This data supports the therapeutic possibility of curcumin use in antioxidant therapy for ARLD, since ethanol is implicated in the loss of antioxidant capacity and increases in oxidative stress. Taken together, this data suggests that both free antioxidant compounds and entrapped compounds provide beneficial effects on protecting against oxidative stress in an ARLD model.

Whilst curcumin nanoformulations have shown promise in a number of *in vitro* and *in vivo* studies^{78,79} this is now being translated into clinical investigations. For example, treatment of patients undergoing coronary elective angioplasty with curcumin nanoformulations showed lower indicators of oxidative injury⁸⁰, whereas, protective effects with curcumin nanoformulations during cancer treatment has been demonstrated in a number of cancers⁸¹. Furthermore, there are ongoing clinical trials examining curcumin nanoformulations in

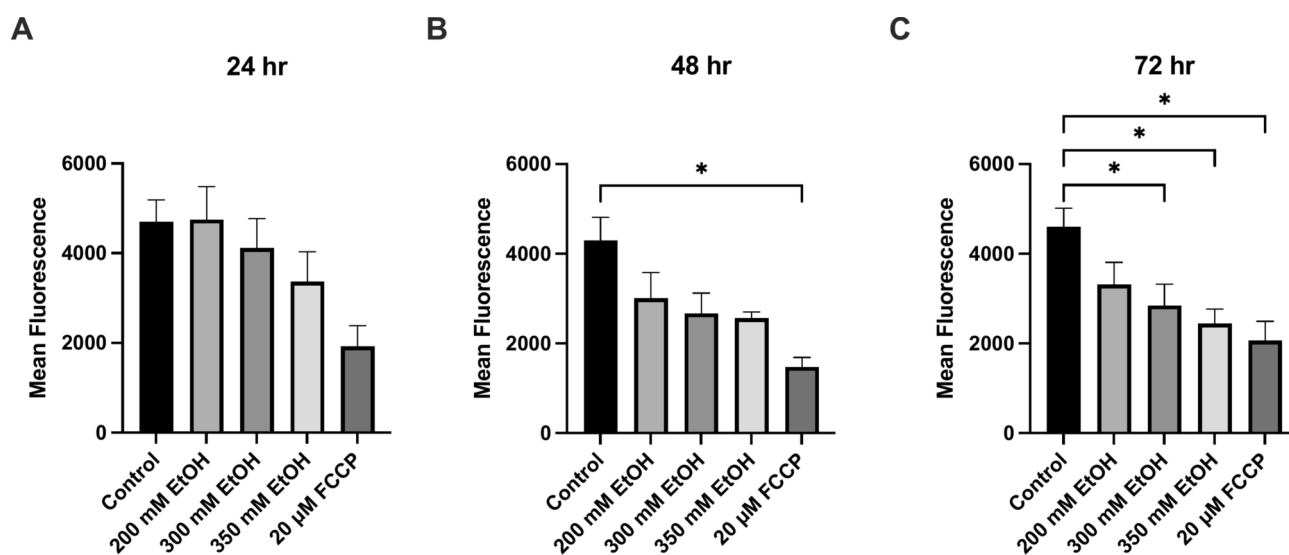


Fig. 4. The effect of ethanol on mitochondrial membrane potential at (A) 24 h, (B) 48 h and (C) 72 h. FCCP (20 μM) was used as a positive control. Data is presented as mean fluorescence values. Results presented as mean of replicates \pm SEM ($n = 3$). * $P < 0.05$.

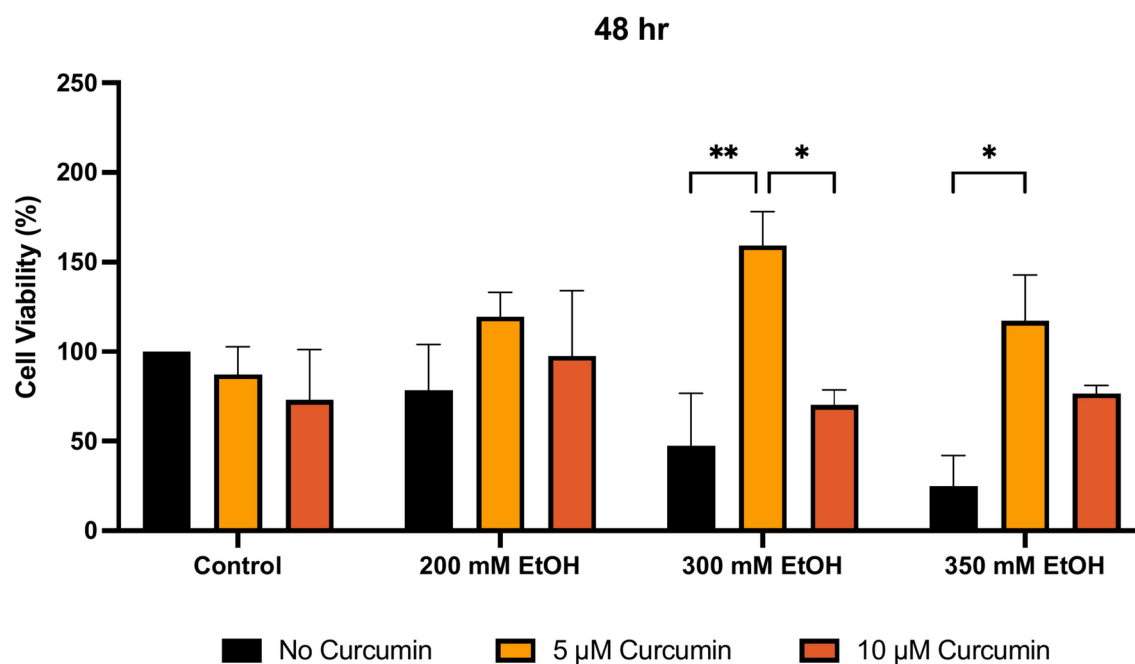
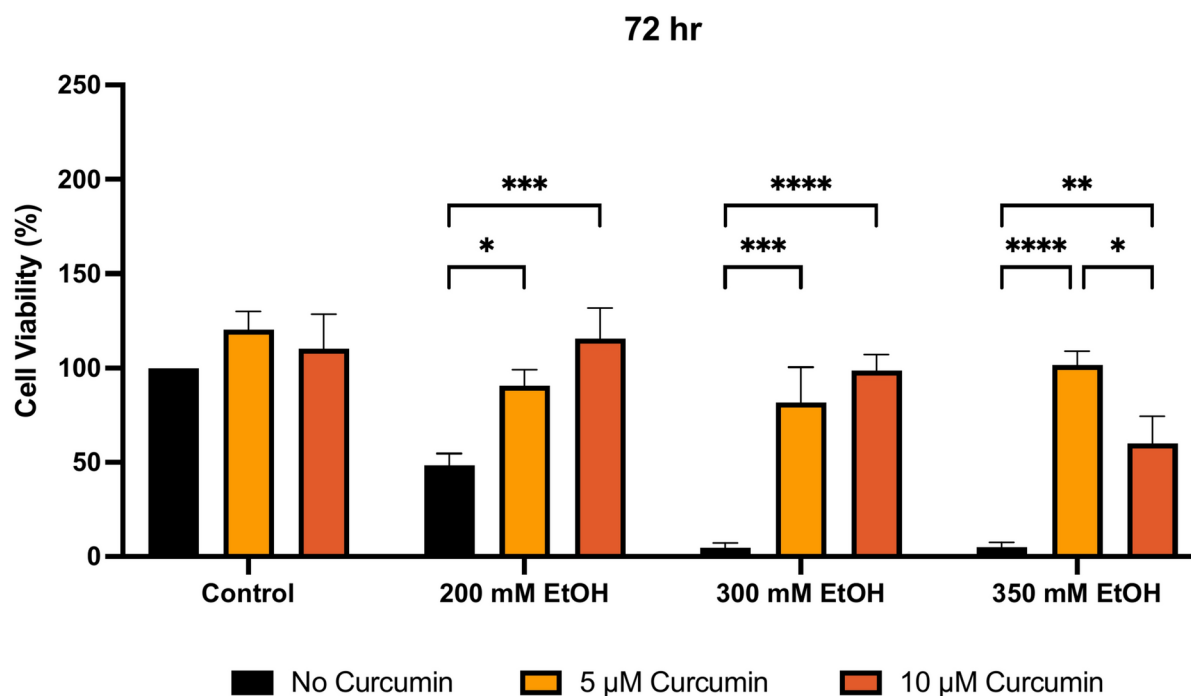
A**B**

Fig. 5. The effect of curcumin free drug co-treatment with and ethanol on cell viability at (A) 48 h and (B) 72 h. Cells were seeded in 96-well plates and co-treated with ethanol and curcumin. Viability was determined by MTT assay. Data is presented as percentage from the control. Results presented as mean + SEM ($n = 3$) * $P \leq 0.05$, ** $P \leq 0.01$, *** $P \leq 0.001$, **** $P \leq 0.0001$.

colon cancer (NCT01294072). Despite this, there are a number of challenges that lie ahead. Whilst the dose of curcumin has been shown to be safe in a number of clinical studies, long term usage remains to be determined.

There are number of limitations in the current study. Whilst we only focussed on 350 mM alcohol treatment when studying curcumin nanoformulations, it would be useful to examine varying concentrations of alcohol from

Active ingredient (10 mg)	Polymer (100 mg)	d (nm)	PDI	Zeta potential (mV)	DL (%)	EE (%)
Curcumin	100% DSPE-PEG	8.40 ± 0.67	0.43 ± 0.03	- 15.20 ± 0.95	7.11 ± 0.00	78.25 ± 0.02

Table 1. Nanoformulation characteristics. Hydrodynamic diameter (d), polydispersity index (PDI), surface charge, drug loading (DL) and encapsulation efficiency (EE) of curcumin DSPE-PEG nanoformulations prepared at 80 °C (mean ± SEM n = 3).

100 mM combined with curcumin formulations. In addition, further examination of inflammatory pathways, including studying antioxidant levels such as GSH will provide further information into the mechanisms of protection provided by curcumin. Finally, we need to undertake *in-vitro* studies beyond three days. Future improvements include evaluation of other antioxidant based nanoformulations, such as NAC, and translation of *in-vitro* findings to *in-vivo* models, and preclinical studies.

Conclusion

Overall, this study observed that exposure to ethanol resulted in notable cellular toxicity, particularly pronounced at higher concentrations of ethanol. Additionally, ethanol treatment led to increases in the production of ROS and apoptosis, indicating a distinct correlation between alcohol consumption and levels of oxidative stress. The study further identified disruptions to mitochondrial regulation following alcohol treatment, including reductions in mitochondrial membrane potential. Consequently, mitochondrial dysregulation as well as mitochondrial damage caused by alcohol has the potential to impede cellular energy production and contribute to apoptosis. This study demonstrates for the first time that successful entrapment of curcumin into DSPE-PEG carriers provides protection against oxidative stress in a cellular model of ARLD. These results show that ethanol causes significant reduction in cell viability and increases ROS production. Treatment with carrier entrapped antioxidants was able to enhance or match the protective effects of the free drugs. This study demonstrates evidence for the use of nanoformulated antioxidants in the treatment of ARLD. However, further investigations are required to assess the ability of these formulations to protect against other parameters of ARLD.

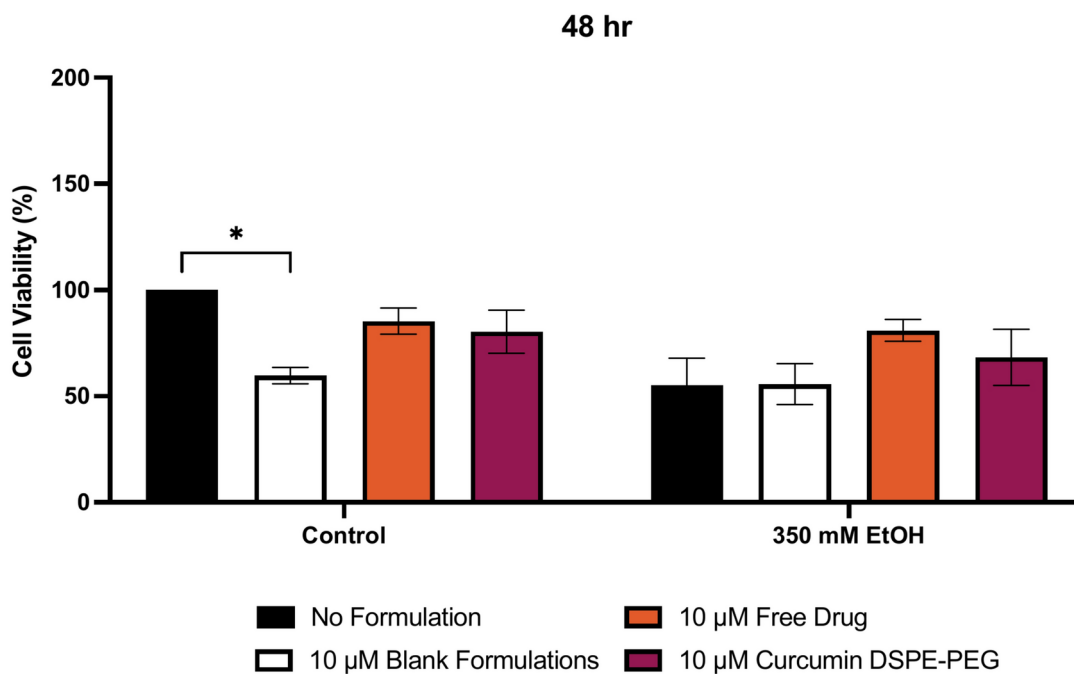
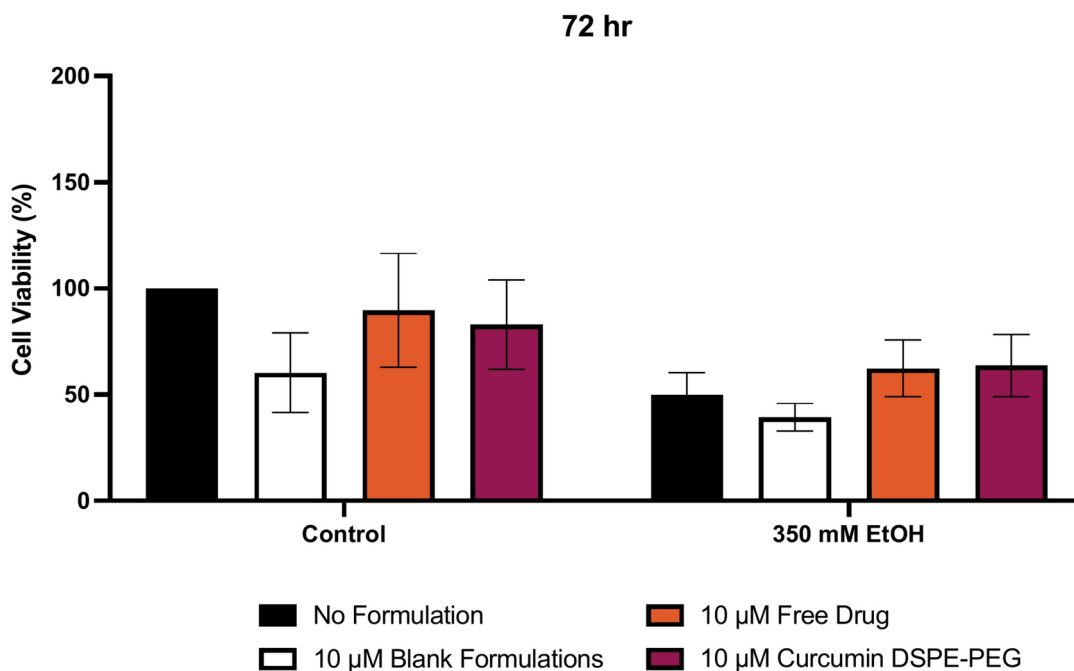
A**B**

Fig. 6. 3-h pre-treatment with nanoformulated curcumin on loss of cell viability at (A) 48 h and (B) 72 h. Cells were seeded in 96-well plates and treated with 350 mM ethanol after 3 h pre-treatment of formulations. Viability of cells was determined by an MTT assay and measured at 48 h and 72 h. Data is presented as percentage from the control. Results presented as mean \pm SEM (n = 3) *P \leq 0.05.

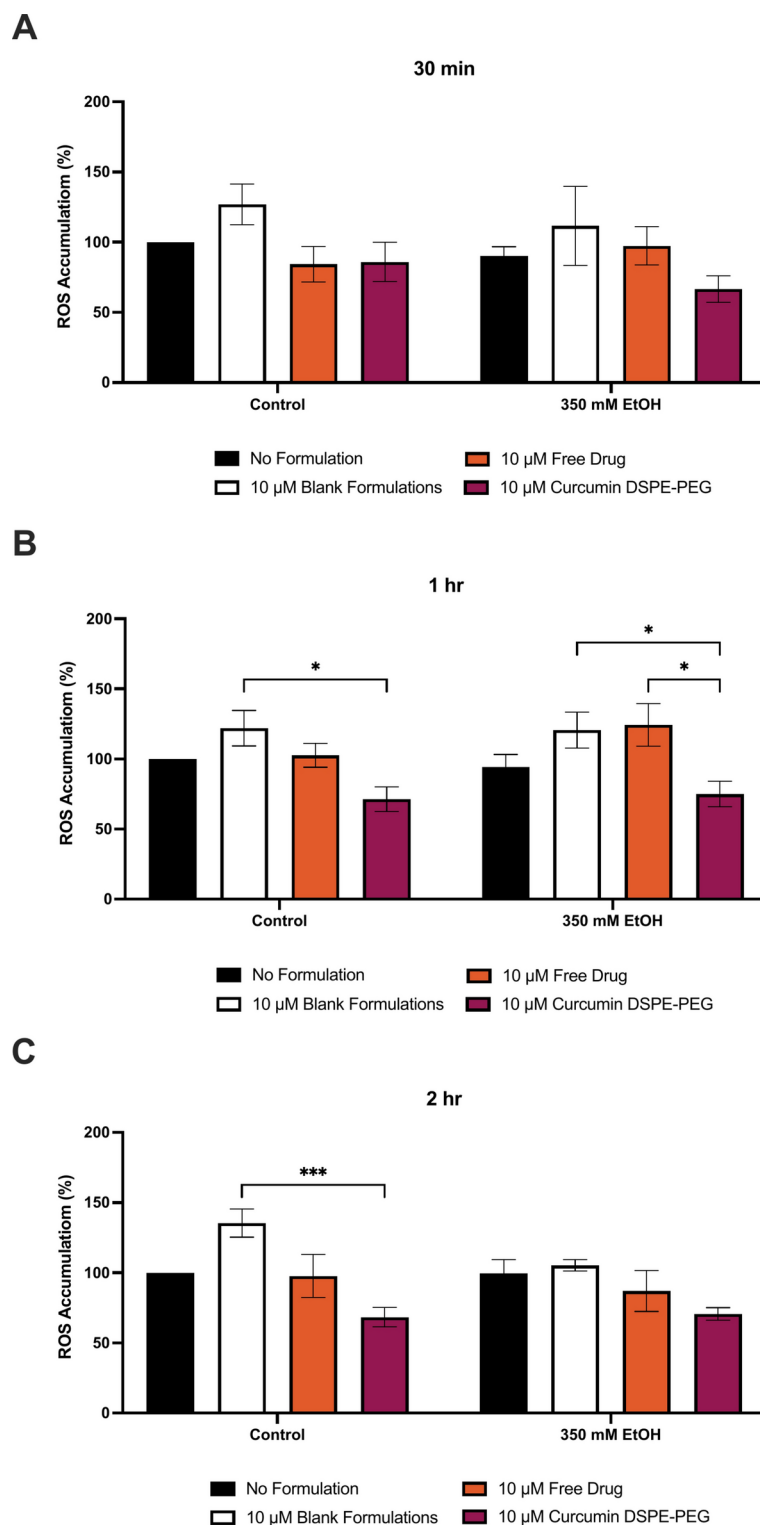


Fig. 7. 3 h pre-treatment of nanoformulated curcumin on ethanol induced ROS production at (A) 30 min, (B) 1 h and (C) 2 h. Cells were seeded in 96-well plates and treated with 350 mM ethanol after 3 h pre-treatment of formulations. ROS production was determined by the DCFDA assay. Data is presented as percentage from the control. Results presented as mean + SEM (n = 3) *P \leq 0.05, ***P \leq 0.001.

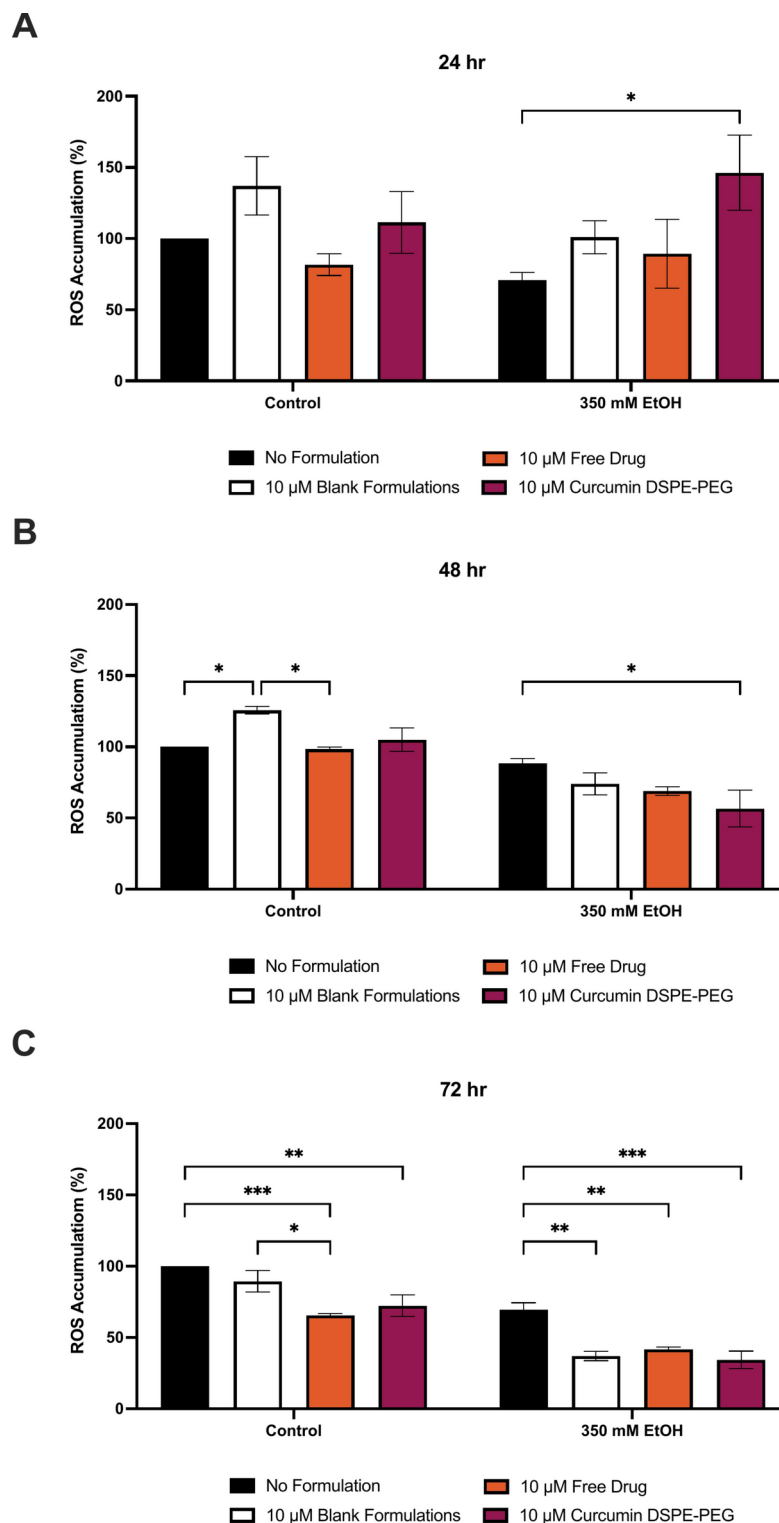


Fig. 8. 3 h pre-treatment of nanoformulated curcumin on ethanol induced ROS production at (A) 24 h, (B) 48 h and (C) 72 h. Cells were seeded in 96-well plates and treated with 350 mM ethanol after 3 h pre-treatment of formulations. ROS production was determined by the DCFDA assay. Data is presented as percentage from the control. Results presented as mean + SEM (n = 3) *P ≤ 0.05, **P ≤ 0.01, ***P ≤ 0.001.

Data availability

The datasets used and/or analysed during the current study are available from the corresponding author upon reasonable request.

Received: 17 June 2024; Accepted: 18 February 2025

Published online: 05 March 2025

References

- Mathurin, P. et al. EASL clinical practical guidelines: Management of alcoholic liver disease. *J. Hepatol.* **57**, 399–420 (2012).
- Devarbhavi, H., Asrani, S. K., Arab, J. P., Nartey, Y. A., Pose, E., Kamath, P. S. Global burden of liver disease: 2023 Update. *J. Hepatol.* <https://doi.org/10.1016/j.jhep.2023.03.017> (2023).
- WHO. Global status report on alcohol and health 2018. <https://apps.who.int/iris/bitstream/handle/10665/274603/9789241565639-eng.pdf?ua=1>.
- Lucey, M. R., Mathurin, P. & Morgan, T. R. Alcoholic hepatitis. *N. Engl. J. Med.* **360**, 2758 (2009).
- Cichoż-Lach, H. & Michalak, A. Oxidative stress as a crucial factor in liver diseases. *World J. Gastroenterol.* **20**, 8082–8091 (2014).
- Tiniakos, D. G., Anstee, Q. M., Burt, A. D. Fatty liver disease. In *MacSween's Pathology of the Liver* 308–371 (Elsevier, 2018).
- Heymann, H. M., Gardner, A. M. & Gross, E. R. Aldehyde-induced DNA and protein adducts as biomarker tools for alcohol use disorder. *Trends Mol. Med.* **24**, 144–155 (2018).
- Ayala, A., Muñoz, M. F., Argüelles, S. Lipid peroxidation: production, metabolism, and signaling mechanisms of malondialdehyde and 4-hydroxy-2-nonenal. *Oxid. Med. Cell Longev.* **2014**. <https://doi.org/10.1155/2014/360438> (2014).
- Petagine, L., Zariwala, M. G. & Patel, V. B. Alcoholic liver disease: Current insights into cellular mechanisms. *World J. Biol. Chem.* **12**, 87–103 (2021).
- Zhou, Y., Wu, R., Wang, X., Bao, X. & Lu, C. Roles of necroptosis in alcoholic liver disease and hepatic pathogenesis. *Cell Prolif.* **55**, e13193 (2022).
- Schwabe, R. F. & Luedde, T. Apoptosis and necroptosis in the liver: a matter of life and death. *Nat. Rev. Gastroenterol. Hepatol.* **15**, 738–752 (2018).
- Kawaratani, H. et al. The effect of inflammatory cytokines in alcoholic liver disease. *Mediat. Inflamm.* <https://doi.org/10.1155/2013/495156> (2013).
- Nagy, L. E. The role of innate immunity in alcoholic liver disease. *Alcohol Res.* **37**, 237–250 (2015).
- Pessione, F. et al. Five-year survival predictive factors in patients with excessive alcohol intake and cirrhosis. Effect of alcoholic hepatitis, smoking and abstinence. *Liver Int.* **23**, 45–53 (2003).
- Brunt, P. W., Kew, M. C., Scheuer, P. J. & Sherlock, S. Studies in alcoholic liver disease in Britain: 1 Clinical and pathological patterns related to natural history. *Gut.* **15**, 52–58 (1974).
- Miller, W. R., Walters, S. T. & Bennett, M. E. How effective is alcoholism treatment in the United States?. *J. Stud. Alcohol.* **62**, 211–220 (2001).
- Frazier, T. H., Stocker, A. M., Kershner, N. A., Marsano, L. S. & McClain, C. J. Treatment of alcoholic liver disease. *Therap. Adv. Gastroenterol.* **4**, 63–81 (2011).
- Hughes, E., Hopkins, L. J. & Parker, R. Survival from alcoholic hepatitis has not improved over time. *PLoS One.* **13**, e0192393 (2018).
- Louvet, A. et al. Effect of prophylactic antibiotics on mortality in severe alcohol-related hepatitis: a randomized clinical trial. *JAMA.* **329**, 1558–1566 (2023).
- Forrest, E. et al. Steroids or pentoxifylline for alcoholic hepatitis (STOPAH): study protocol for a randomised controlled trial. *Trials.* **14**, 262 (2013).
- Forrest, E. H. et al. Application of prognostic scores in the STOPAH trial: Discriminant function is no longer the optimal scoring system in alcoholic hepatitis. *J. Hepatol.* **68**, 511–518 (2018).
- Bartneck, M., Warzecha, K. T. & Tacke, F. Therapeutic targeting of liver inflammation and fibrosis by nanomedicine. *Hepatobiliary Surg. Nutr.* **3**, 364–36476 (2014).
- Petagine, L., Everitt, H., Preedy, V., Sherwood, R. & Patel, V. Acute alcohol tissue damage: protective properties of betaine. *J. Ren. Hepatic Disord.* **5**, 19–29 (2021).
- Yan, J., Nie, Y., Luo, M., Chen, Z. & He, B. Natural compounds: a potential treatment for alcoholic liver disease?. *Front. Pharmacol.* **12**, 1695 (2021).
- Bai, X., Su, G. & Zhai, S. Recent advances in nanomedicine for the diagnosis and therapy of liver fibrosis. *Nanomaterials.* **10**, 1–18 (2020).
- Mursaleen, L., Somavarapu, S. & Zariwala, M. G. Deferoxamine and curcumin loaded nanocarriers protect against rotenone-induced neurotoxicity. *J. Parkinsons Dis.* **10**, 99–111 (2020).
- Wu, H. et al. Metabolic basis of ethanol-induced cytotoxicity in recombinant HepG2 cells: Role of nonoxidative metabolism. *Toxicol. Appl. Pharmacol.* **216**, 238–247 (2006).
- Kumar, S. M. et al. The effects of changes in glutathione levels through exogenous agents on intracellular cysteine content and protein adduct formation in chronic alcohol-treated VL17A cells. *Toxicol. Mech. Methods.* **27**, 128–135 (2017).
- Donohue, T. M., Osna, N. A. & Clemens, D. L. Recombinant Hep G2 cells that express alcohol dehydrogenase and cytochrome P450 2E1 as a model of ethanol-elicited cytotoxicity. *Int. J. Biochem. Cell Biol.* **38**, 92–101 (2006).
- Valdés-Arzate, A. et al. Hepatocyte growth factor protects hepatocytes against oxidative injury induced by ethanol metabolism. *Free Radic. Biol. Med.* **47**, 424–430 (2009).
- Ghazali, R. et al. High omega arachidonic acid/docosahexaenoic acid ratio induces mitochondrial dysfunction and altered lipid metabolism in human hepatoma cells. *World J. Hepatol.* **12**, 84–98 (2020).
- Lu, Y. & Cederbaum, A. I. CYP2E1 and oxidative liver injury by alcohol. *Free Radic. Biol. Med.* **44**, 723–738 (2008).
- Cederbaum, A. I., Lu, Y. & Wu, D. Role of oxidative stress in alcohol-induced liver injury. *Arch. Toxicol.* **83**, 519–548 (2009).
- Gyamfi, D., Everitt, H. E., Tewfik, I., Clemens, D. L. & Patel, V. B. Hepatic mitochondrial dysfunction induced by fatty acids and ethanol. *Free Radic. Biol. Med.* **53**, 2131–2145 (2012).
- Kim, W., Jeong, H.-S., Kim, S.-C., Choi, C.-H. & Lee, K.-H. Chronic alcohol exposure of cells using controlled alcohol-releasing capillaries. *Cells.* <https://doi.org/10.3390/cells10051120> (2021).
- She, X. et al. In vitro antioxidant and protective effects of corn peptides on ethanol-induced damage in HepG2 cells. *Food Agric. Immunol.* **27**, 99–110 (2016).
- Qian, Z.-J. et al. Intracellular ethanol-mediated oxidation and apoptosis in HepG2/CYP2E1 cells impaired by two active peptides from seahorse (*Hippocampus kuda bleeler*) protein hydrolysates via the Nrf2/HO-1 and akt pathways. *Food Sci. Nutr.* **9**, 1584–1602 (2021).
- Yang, C.-F. et al. NOX4/ROS mediate ethanol-induced apoptosis via MAPK signal pathway in L-02 cells. *Int. J. Mol. Med.* **41**, 2306–2316 (2018).
- Na, A.-Y. et al. Protective effect of isoliquiritigenin against ethanol-induced hepatic steatosis by regulating the SIRT1-AMPK pathway. *Toxicol. Res.* **34**, 23–29 (2018).
- Stoica, S. I. et al. Molecular aspects of hypoxic stress effects in chronic ethanol exposure of neuronal cells. *Curr. Issues Mol. Biol.* **45**, 1655–1680 (2023).
- Clemens, D. L., Halgard, C. M., Miles, R. R., Sorrell, M. F. & Tuma, D. J. Establishment of a recombinant hepatic cell line stably expressing alcohol dehydrogenase. *Arch. Biochem. Biophys.* **321**, 311–318 (1995).

42. Baldini, P. et al. Atrial natriuretic peptide effects on intracellular pH changes and ROS production in HEPG2 cells: role of p38 MAPK and phospholipase D. *Cell Physiol. Biochem.* **15**, 077–088 (2005).
43. Bradford, M. M. A rapid and sensitive method for the quantitation of microgram quantities of protein utilizing the principle of protein-dye binding. *Anal. Biochem.* **72**, 248–254 (1976).
44. Fenech, M. Cytokinesis-block micronucleus cytome assay. *Nat. Protoc.* **2**, 1084–1104 (2007).
45. Mursaleen, L., Chan, S. H. Y., Noble, B., Somavarapu, S. & Zariwala, M. G. Curcumin and N-acetylcysteine nanocarriers alone or combined with deferoxamine target the mitochondria and protect against neurotoxicity and oxidative stress in a co-culture model of Parkinson's disease. *Antioxidants (Basel, Switzerland)*. <https://doi.org/10.3390/antiox12010130> (2023).
46. Shahiduzzaman, M., Dyachenko, V., Khalafalla, R. E., Desouky, A. Y. & Dausgschies, A. Effects of curcumin on *Cryptosporidium parvum* in vitro. *Parasitol. Res.* **105**, 1155–1161 (2009).
47. Premanand, C., Rema, M., Sameer, M. Z., Sujatha, M. & Balasubramanyam, M. Effect of curcumin on proliferation of human retinal endothelial cells under in vitro conditions. *Investig. Ophthalmol. Vis. Sci.* **47**, 2179–2184 (2006).
48. Tyrrell, Z. L., Shen, Y. & Radosz, M. Fabrication of micellar nanoparticles for drug delivery through the self-assembly of block copolymers. *Prog. Polym. Sci.* **35**, 1128–1143 (2010).
49. Somavarapu, S. et al. Engineering artesunate-loaded micelles using spray drying for pulmonary drug delivery. *J. Drug Deliv. Sci. Technol.* **86**, 104641 (2023).
50. Zariwala, M. G., Farnaud, S., Merchant, Z., Somavarapu, S. & Renshaw, D. Ascorbyl palmitate/DSPE-PEG nanocarriers for oral iron delivery: Preparation, characterisation and in vitro evaluation. *Colloids Surf. B Biointerfaces.* **115**, 86–92 (2014).
51. Moribe, K. et al. Ascorbyl dipalmitate/PEG-lipid nanoparticles as a novel carrier for hydrophobic drugs. *Int. J. Pharm.* **387**, 236–243 (2010).
52. Mursaleen, L., Noble, B., Chan, S. H. Y., Somavarapu, S. & Zariwala, M. G. N-Acetylcysteine nanocarriers protect against oxidative stress in a cellular model of Parkinson's disease. *Antioxidants* **9**, 600 (2020).
53. Schiano, E. et al. Antioxidant and antidiabetic properties of a thinned-nectarine-based nanoformulation in a pancreatic β -cell line. *Antioxidants*. <https://doi.org/10.3390/antiox13010063> (2024).
54. Chan, S. H. Y., Sheikh, K., Zariwala, M. G. & Somavarapu, S. Dry powder formulation of azithromycin for COVID-19 therapeutics. *J. Microencapsul.* **40**, 217–232 (2023).
55. Louvet A, hepatology PM-N reviews G&, 2015 undefined. Alcoholic liver disease: mechanisms of injury and targeted treatment. <https://www.nature.com/nrgastro/journal/v12/n4/abs/nrgastro.2015.35.html> (accessed 13 Nov 2019).
56. Rastovic, U. et al. Human precision-cut liver slices: a potential platform to study alcohol-related liver disease. *Int. J. Mol. Sci.* <https://doi.org/10.3390/ijms25010150> (2024).
57. Zhao, R. Z., Jiang, S., Zhang, L. & Yu, Z. B. Mitochondrial electron transport chain, ROS generation and uncoupling (Review). *Int. J. Mol. Med.* **44**, 3–15 (2019).
58. Osna, N. A., Donohue, T. M. & Kharbanda, K. K. Alcoholic liver disease: pathogenesis and current management. *Alcohol Res.* **38**, 147–161 (2017).
59. Hoek, J. B., Cahill, A. & Pastorino, J. G. Alcohol and mitochondria: A dysfunctional relationship. *Gastroenterology.* **122**, 2049–2063 (2002).
60. Cooper, I. D., Kyriakidou, Y., Petagine, L., Edwards, K. & Elliott, B. T. Bio-hacking better health—leveraging metabolic biochemistry to maximise healthspan. *Antioxidants*. <https://doi.org/10.3390/antiox12091749> (2023).
61. Wang, K. Molecular mechanisms of hepatic apoptosis. *Cell Death Dis.* **5**, e996–e996 (2014).
62. Viña, J., Estrela, J. M., Guerri, C. & Romero, F. J. Effect of ethanol on glutathione concentration in isolated hepatocytes. *Biochem. J.* **188**, 549–552 (1980).
63. Anthony, B., Zhou, F. C., Ogawa, T., Goodlett, C. R. & Ruiz, J. Alcohol exposure alters cell cycle and apoptotic events during early neurogenesis. *Alcohol Alcohol.* **43**, 261–273 (2008).
64. Benassi-Evans, B. & Fenech, M. Chronic alcohol exposure induces genome damage measured using the cytokinesis-block micronucleus cytome assay and aneuploidy in human B lymphoblastoid cell lines. *Mutagenesis.* **26**, 421–429 (2011).
65. Fenech, M. et al. Micronuclei as biomarkers of DNA damage, aneuploidy, inducers of chromosomal hypermutation and as sources of pro-inflammatory DNA in humans. *Mutat. Res. Mutat. Res.* **786**, 108342 (2020).
66. Hyun, J., Han, J., Lee, C., Yoon, M. & Jung, Y. Pathophysiological aspects of alcohol metabolism in the liver. *Int. J. Mol. Sci.* <https://doi.org/10.3390/ijms22115717> (2021).
67. Farfán Labonne, B. E. et al. Acetaldehyde-induced mitochondrial dysfunction sensitizes hepatocytes to oxidative damage. *Cell Biol. Toxicol.* **25**, 599–609 (2009).
68. Petagine, L., Everitt, H., Sherwood, R., Gyamfi, D. & Patel, V. B. Time-dependent alterations in liver oxidative stress due to ethanol and acetaldehyde. *J. Ren. Hepatic Disord.* **6**, 56–66 (2022).
69. Patel, V. B. et al. Cardioprotective effect of propranolol from alcohol-induced heart muscle damage as assessed by plasma cardiac troponin-T. *Alcohol Clin. Exp. Res.* **25**, 882–889 (2001).
70. Kunnumakkara, A. B. et al. Curcumin, the golden nutraceutical: multitargeting for multiple chronic diseases. *Br. J. Pharmacol.* **174**, 1325–1348 (2017).
71. Pourbagher-Shahri, A. M., Farkhondeh, T., Ashrafzadeh, M., Talebi, M. & Samarghandian, S. Curcumin and cardiovascular diseases: Focus on cellular targets and cascades. *Biomed. Pharmacother.* **136**, 111214 (2021).
72. Garodia, P., Hegde, M., Kunnumakkara, A. B., Aggarwal, B. B. Curcumin, inflammation, and neurological disorders: how are they linked? *Integr. Med. Res.* 100968 (2023).
73. Rahmani, A. H., Alshahli, M. A., Aly, S. M., Khan, M. A. & Aldebasi, Y. H. Role of curcumin in disease prevention and treatment. *Adv. Biomed. Res.* **7**, 38 (2018).
74. Jabczyk, M., Nowak, J., Hudzik, B. & Zubelewicz-Szkodzińska, B. Curcumin in metabolic health and disease. *Nutrients*. <https://doi.org/10.3390/nu13124440> (2021).
75. Machado, I. F., Miranda, R. G., Dorta, D. J., Rolo, A. P. & Palmeira, C. M. Targeting oxidative stress with polyphenols to fight liver diseases. *Antioxidants*. <https://doi.org/10.3390/antiox12061212> (2023).
76. Lukunaprasit, T. et al. An updated meta-analysis of effects of curcumin on metabolic dysfunction-associated fatty liver disease based on available evidence from Iran and Thailand. *Sci. Rep.* **13**, 5824 (2023).
77. Ge, T. et al. The role of the pentose phosphate pathway in diabetes and cancer. *Front. Endocrinol. (Lausanne)*. <https://doi.org/10.3389/fendo.2020.00365> (2020).
78. Amekyeh, H., Alkhader, E., Sabra, R. & Billa, N. Prospects of curcumin nanoformulations in cancer management. *Molecules*. <https://doi.org/10.3390/molecules27020361> (2022).
79. Sun, M. et al. Enhancement of transport of curcumin to brain in mice by poly(n-butylcyanoacrylate) nanoparticle. *J. Nanoparticle Res.* **12**, 3111–3122 (2010).
80. Helli, B. et al. Curcumin nanomicelle improves lipid profile, stress oxidative factors and inflammatory markers in patients undergoing coronary elective angioplasty; a randomized clinical trial. *Endocr. Metab. Immune Disord. Drug Targets.* **21**, 2090–2098 (2021).
81. Hegde, M. et al. Nanoformulations of curcumin: An alliance for effective cancer therapeutics. *Food Biosci.* **56**, 103095 (2023).

Acknowledgements

Lucy Petagine was supported by a scholarship from the University of Westminster.

Author contributions

L.P. designed and conducted the experiments, analysed data, and wrote the original draft, designed the figures, and reviewed and edited the final manuscript; M.G.Z. reviewed and edited the manuscript; S.S. prepared nanoformulations and reviewed and edited the final manuscript; S.H.Y.C. prepared and characterised nanoformulations and reviewed and edited the final manuscript; E.S.K. analysed chromosomal instability slides; V.B.P. reviewed and edited the manuscript. All authors have reviewed the manuscript.

Funding

This research received no external funding.

Competing interests

The authors declare no competing interests.

Additional information

Supplementary Information The online version contains supplementary material available at <https://doi.org/10.1038/s41598-025-91139-0>.

Correspondence and requests for materials should be addressed to V.B.P.

Reprints and permissions information is available at www.nature.com/reprints.

Publisher's note Springer Nature remains neutral with regard to jurisdictional claims in published maps and institutional affiliations.

Open Access This article is licensed under a Creative Commons Attribution 4.0 International License, which permits use, sharing, adaptation, distribution and reproduction in any medium or format, as long as you give appropriate credit to the original author(s) and the source, provide a link to the Creative Commons licence, and indicate if changes were made. The images or other third party material in this article are included in the article's Creative Commons licence, unless indicated otherwise in a credit line to the material. If material is not included in the article's Creative Commons licence and your intended use is not permitted by statutory regulation or exceeds the permitted use, you will need to obtain permission directly from the copyright holder. To view a copy of this licence, visit <http://creativecommons.org/licenses/by/4.0/>.

© The Author(s) 2025